Predictive permeability model of faults in crystalline rocks; verification by joint hydraulic factor (JH) obtained from water pressure tests

Hamidreza Rostami Barani*, Gholamreza Lashkaripour and Mohammad Ghafoori

Department of Geology, Ferdowsi University of Mashhad (FUM), Mashhad, Iran.
**Corresponding author. e-mail: ha_barani@yahoo.com*

In the present study, a new model is proposed to predict the permeability per fracture in the fault zones by a new parameter named joint hydraulic factor (JH). JH is obtained from Water Pressure Test (WPT) and modified by the degree of fracturing. The results of JH correspond with quantitative fault zone descriptions, qualitative fracture, and fault rock properties. In this respect, a case study was done based on the data collected from Seyahoo dam site located in the east of Iran to provide the permeability prediction model of fault zone structures. Datasets including scan-lines, drill cores, and water pressure tests in the terrain of Andesite and Basalt rocks were used to analyse the variability of in-site relative permeability of a range from fault zones to host rocks. The rock mass joint permeability quality, therefore, is defined by the JH. JH data analysis showed that the background sub-zone had commonly <3 Lu (less of 5×10^{-5} m^3/s) per fracture, whereas the fault core had permeability characteristics nearly as low as the outer damage zone, represented by 8 Lu (1.3×10^{-4} m^3/s) per fracture, with occasional peaks towards 12 Lu (2×10^{-4} m^3/s) per fracture. The maximum JH value belongs to the inner damage zone, marginal to the fault core, with 14–22 Lu (2.3×10^{-4}–3.6×10^{-4} m^3/s) per fracture, locally exceeding 25 Lu (4.1×10^{-4} m^3/s) per fracture. This gives a proportional relationship for JH approximately 1:4:2 between the fault core, inner damage zone, and outer damage zone of extensional fault zones in crystalline rocks. The results of the verification exercise revealed that the new approach would be efficient and that the JH parameter is a reliable scale for the fracture permeability change. It can be concluded that using short duration hydraulic tests (WPTs) and fracture frequency (FF) to calculate the JH parameter provides a possibility to describe a complex situation and compare, discuss, and weigh the hydraulic quality to make predictions as to the permeability models and permeation amounts of different zone structures.

1. Introduction

Fractures pose a challenge in all types of engineering projects, especially in tunnels, dams, and quarries. The studies carried out in this area showed that the challenges were increased by fracture density, weak rocks, poor rock stability, and enhanced fluid flow (Hoek and Bray 1981; Hoek 2000; Nilsen and Palmstrom 2000; Blindheim and Ovstedal 2001; Gudmundsson 2011; Davoodi *et al.* 2013). The hydraulic conductivity greatly depends on the type of fractures (Pollard and Aydin 1988; Mandal *et al.* 2000, 2004; Gudmundsson 2011; Baruah *et al.* 2013). The classification of fractures is conventionally based on the mode of rock deformation or displacement, which represents a broad mechanical

Keywords. Permeability; fault zones; fracture distribution; water pressure test (WPT); joint hydraulic factor (JH); Seyahoo dam.

classification (Pollard and Aydin 1988): (I) Dilatant fractures, (II) Compaction fractures, and (III) Shear fractures/faults. There are several models to define 'zones', primarily focusing on fault zones. Caine *et al.* (1996) present a conceptual model to classify the conductivity structures in fault zones (figure 1). A similar approach to define deformation zone architecture is adopted by Munier *et al.* (2003). Both approaches define the zone as a core area (fault core) with a transition zone (damage zone) to the undisturbed host rock (protolith). The brackets indicate the nomenclature used by Caine *et al.* (1996). The established terminologies on fault zone architecture in metamorphic and crystalline rocks (Caine *et al.* 1996; Seront *et al.* 1998) are the fault core, damage zone, and protolith. Fault models outline a core that has undergone the main part of displacement, and is therefore hosting fault rocks. Deformation, moreover, is mainly accommodated by fractures of the damage zone. The boundary between the core and damage zone is typically sharp, and is defined by slip surfaces (shear fractures), whereas the transition between the damage zone and protolith is marked by a decrease in fracture intensity to a regional background frequency level. These models predict a zoned permeability field in fault zones in crystalline rocks (Caine *et al.* 1996; Evans *et al.* 1997; Wibberley and Shimamoto 2003; Walker *et al.* 2013), where a low permeability fault core is typically surrounded by a more permeable damage zone towards pristine, lower or impermeable host rocks. Protolith rocks have negligible primary porosity and permeability unless damaged by brittle deformation (Norton and Knapp 1977; Morrow and Byerlee 1988; 1992; Morrow and Lockner 1997).

The fracture intensity shows a significant increase in frequency from the background level towards the fault core in the damage zone (Caine *et al.* 1996; Braathen *et al.* 1998). Not only the frequency but also the length of fractures is of interest. As a key conclusion drawn from simulation of flow in fracture systems, long fractures will conduct more water than short fractures, due to higher connectivity (Odling 1997; Babiker and Gudmundsson 2004; Masumoto *et al.* 2007; Mitchell and Faulkner 2012). Detailed analyses of the damage zones reveal subzones characterized by distinct fracture sets and populations, as outlined in Braathen *et al.* (2004). They describe a core of fault rocks surrounding lenses of host rock with a dense network (20–100 f/m) of short fractures. The damage zone which is connected by shorter fractures has an inner part, 5–50 m wide, dominated by fault-parallel, moderate frequency long fractures. This, in total, gives an appropriate connectivity. The outer part of the damage zone shows decreasing frequency of fractures, which vary in length and orientation, demarcating the transition from damage zone to background fracture level.

Permeability models of faults combine numerical simulations with laboratory permeability measurements (Morrow and Byerlee 1988, 1992; Morrow and Lockner 1997; Seront *et al.* 1998; Faulkner and Rutter 2001). Recent studies confirm that the permeability of rocks and fractures is reduced with depth, i.e., with increasing effective pressure in 10 m below the surface or the parts 100 m deeper (Morrowand Byerlee 1988, 1992; Morrow and Lockner 1997; Gudmundsson 2011). The findings are supported by studies on permeability studies aimed to examine faults at shallow depth showing that the lowest permeability is found in the fault core, as addressed by Seront *et al.* (1998). The results of laboratory and field studies reveal that the damage zone is characterized with greater fluid conduction due to its higher permeability rates, which are several times greater than those of the

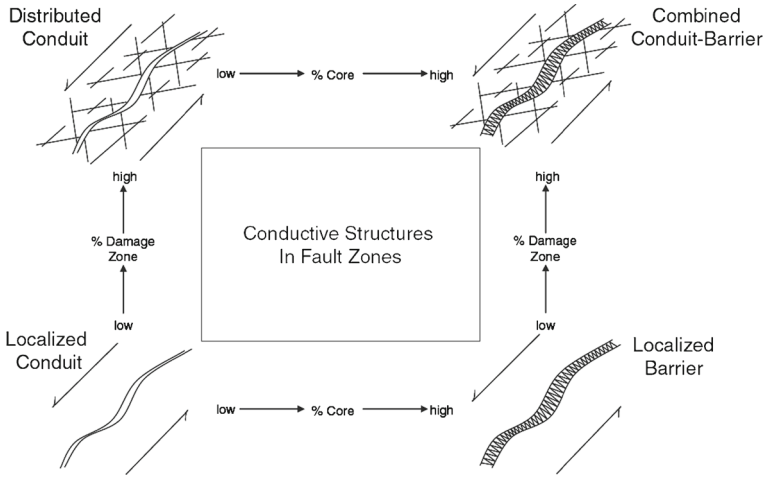

Figure 1. Conceptual scheme for conductivity structures in 'zones' modified according to Caine *et al.* (1996).

protolith and the core (Babiker and Gudmundsson 2004). These results are undermined by Faulkner and Rutter (2001), who questioned the value of the results of the laboratory test in which the natural fault rocks are not intact with *in situ* fabrics. However, Evans *et al.* (1997) conclude that there is a permeability contrast between fault core and damage zone to the magnitude of 10–10^4, with a maximum contrast of 10^6. Furthermore, they argue that the permeability field is anisotropic to an order of 10^4, with the highest permeability parallel to the fault.

Most of the problems in rock permeability analysis require reliable knowledge of hydro-mechanical properties of the joint plane to be solved. The permeability of the rock mass was calculated in the sections per meter of the length regardless of the characteristics of the joints. Hydraulic tests, for example, were performed in sections of equal length. It was found that some sections were tight while others were conductive. Consequently, it is necessary to modify water pressure tests on the basis of a number of conductive fractures. In this study, fault rock descriptions related to polyphase activities during faulting and unroofing were combined with damage zone fracture properties based on technical data. The uniqueness of the following study lies in the connection between structural observations linked with joint hydraulic factor (JH) in Seyahoo dam. A different JH quality type was observed in the fault zone. The paper presents permeability analysis based on JH which predicts permeability of fracture in the fault zone, which opens for *in situ* considerations of the permeability structure of fault zones.

2. Joint hydraulic factor (JH) concept

From a grouting perspective, the joint system of the rock mass is conductive, rather than the intact rock. Figure 2 illustrates the approach. A borehole section is either considered tight or conductive. The hydraulic quality is defined by the joint hydraulic factor (JH). In this respect, hydraulics of the water paths (N_h) have a special importance. The joint trace length and hydraulic aperture are perhaps significant properties of the joint plane in the quality of the JH. A sheer number of studies on conductive joints (N_h) in relation to the total number of joints (FF) were performed in bore holes by Axelsson and Turesson (1996). The frequency of conductive joints was reported to be between 5 and 25% (N_h = 5–25% FF) and the best trend line was $N_h = 0.977\text{FF}^{0.59}$ (Rostami Barani 2013).

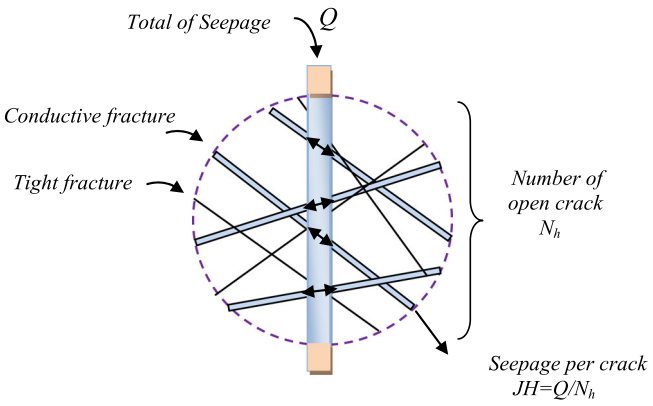

Figure 2. Illustration of the JH factor concept obtained from water pressure test (WPT).

3. Methods and datasets

A combination of field, micro structural, and experimental static permeability characterizations is used to determine fault permeability structure evolution in fault zones. Presented datasets include scan-lines, drill cores and water pressure tests of boreholes in Seyahoo dam. The general characteristics of the rock mass are described as follows:

3.1 *Measured fracture frequency (FF)*

The main dataset on structures is obtained from drill cores, which implies the classification of the rock mass quality and its subordinate part is based on this dataset. Note that the fracture frequency (FF) in drill cores is regarded higher than *in situ* FF due to the applied stress during drilling. Measuring true aperture or orientation of fractures in the drill cores was not viable due to mobility of the cores during drilling and within the storage boxes. Furthermore, the drill cores are not oriented. The coverage of drill cores is locally variable and drill cores have not been collected and/or stored, especially along stretches of unfractured host rock. In addition, where the rock is of poor quality, as in fault cores, core loss is a common phenomenon. To quantify the rock zones, and for plotting purposes, class values of FF were pre-set for occurrence of (noncohesive) fault rocks, representing breccia (50 f/m) or gouge (70 f/m). All frequencies below these thresholds are measured, and values below this level represent actual FF.

3.2 *Calculated permeability*

The water pressure test (WPT) (in which pressurised water is injected into the borehole) is an effective field test of rock mass permeability and is mostly conducted using the Lugeon method. The

water take (discharge) is measured under increasing (loading) and decreasing (unloading) pressure steps (the amount of pressure changed) at proper time intervals along the borehole. The packer test is used for isolated sections between expandable double packers or between a single packer and the bottom of a borehole. To seal off a test section from other parts of the borehole, packer rubbers should be pressurized and then expanded against the borehole wall. Water is injected into the test section and then the water pressure is measured. The following factors influence the test results: the presence of the fractures or a fracture zone, the fracture distribution pattern, the length of test interval, and the effect of the artificial water table, streams, lakes or rivers. The test fails if leakage from packers takes place, the borehole is improperly flushed, head loss is not accounted for, or hydraulic fracturing occurs (Mollah and Sayed 1995). The water pressure test or Lugeon permeability test is the most common and appropriate method in order to determine rock mass permeability due to the presence of weak planes, such as faults, bedding planes, joints, fissure, etc. (USACE 1993; Lashkaripour and Ghafoori 2002). According to Nonveiller (1989), the Lu value may be:

$$\mathrm{Lu} = \frac{VP_s}{TP_iL}, \tag{1}$$

where V is the water takes (L), P_s is the standard injection pressure (981 kPa), T is the injection time (min), P_i is the injection pressure used (kPa), L is the length of grout section (m) and Lu is the Lugeon coefficient: water absorption (l/min/m).

At present, it is broadly accepted that the water pressure test can induce modifications in the degree of jointing (Shibata 1981; Kutzner 1996; Foyo *et al.* 2005). In rock layers deeper into the underground, the cracks are narrow and comparatively do not take in water because of the greater tectonic stress in lower elevation. The results of this *in situ* test are strongly related to the geometric characteristics and weathering degree of the water paths (Ewert 1997a; Karaguzel and Kilic 2000). The core drilling permits the evaluation of the joint-opening through which water flows, but it does not allow for the definition of the joint continuity. On the other hand, the degree of jointing in the core of boreholes defined by FF constitutes the main reference to predict the test section behaviour under WPT. This index is often employed to decide if the test is necessary or not. The degree of jointing and the water-absorbed quantity should be in a direct relation. However, the rock mass areas having a low jointing degree (fracture frequency) show high water takes, and even a reverse situation is possible.

Obviously, the WPT is not accurate to determine the intact rock permeability. The final objective is to guarantee the accurate sealing of the water paths. In this sense, the hydraulics of the water paths (N_h) has a special importance (Dalmalm 2004). The hydraulic quality is defined by the JH.

$$\mathrm{JH} = \frac{\mathrm{Lu}}{N_h}. \tag{2}$$

4. Results and discussion

4.1 *Investigation site*

The Seyahoo dam, which is a zoned earthfill clay core dam, is 32 m high and 352 m long. The dam is located in the east of Iran in South Khorasan province and is managed by the South Khorasan Water Agency. It provides a barrier for water from the Seyahoo River. The catchment area is approximately 3028 km^2 and the reservoir is 15×10^6 m^3. The dam is flood controlled and capable of supplying the water needed for the regions of downward lands and 700 hectares of Doroh lands (T-MAECO 2013).

A geological cross-section of the dam site was prepared using information from exploration holes (figure 3). The dam foundation is Andesite, and is generally associated with Basalt. Discontinuity planes are constituted by joint sets, faults, and irregular fractures. During the foundation excavations, it was observed that the thickness of fault cores ranges from a few 1–3 m. Fault surfaces are smooth and slicken sided and are composed of fault gouge and breccias. Fracture openings are predominantly filled with clay and calcite. This chronology is confirmed in outcrops of faults on the Seyahoo and in the region, which reveals several types of fault rocks, ranging from semi-ductile mylonites to cataclasites and noncohesive breccias and gouge.

4.2 *Fault zone structure characteristics*

All faults intersected by the dams show a fault zone 60–80 m wide, where the FF commonly increases towards the core of the fault (figure 4). Further, a polyphase history characterized the studied faults, with fault products including impermeable mylonites and cataclasites, which are reworked in porous breccias and gouge. In the Seyahoo dam, the fault cores are narrow in general, seldom exceeding 3 m wide, and characterized by cataclasites superimposed by noncohesive fault rocks. The detailed descriptions of the major faults transected by the dam revealed common fault rocks surrounding intensively fractured rock lenses in

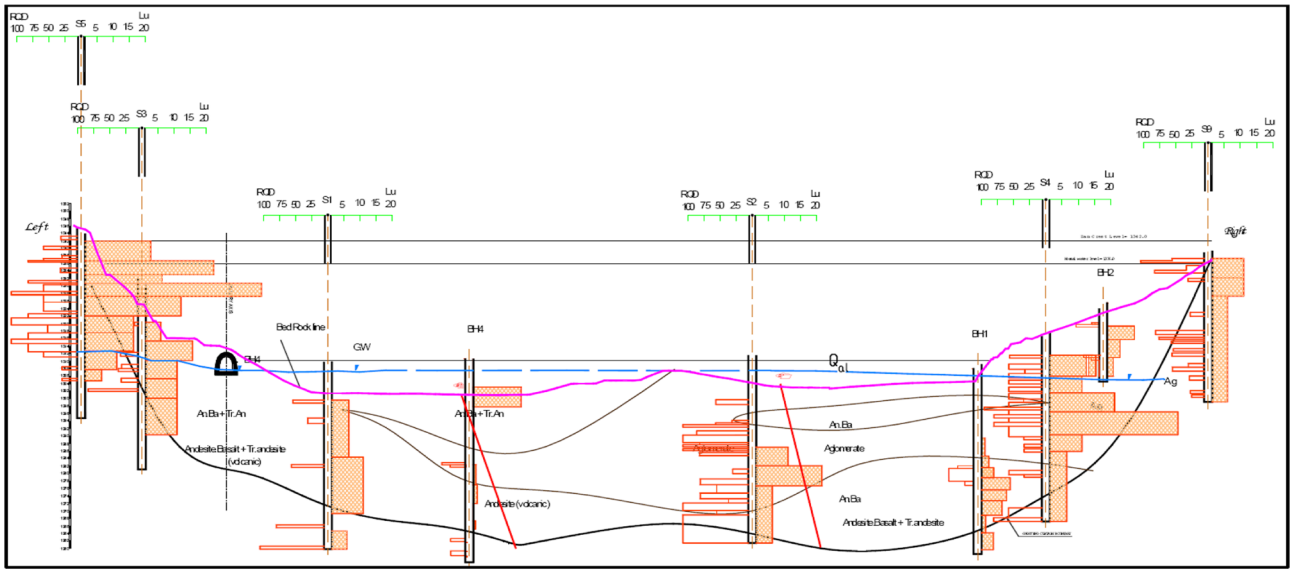

Figure 3. Geological cross-section map of the foundation site of the Seyahoo dam.

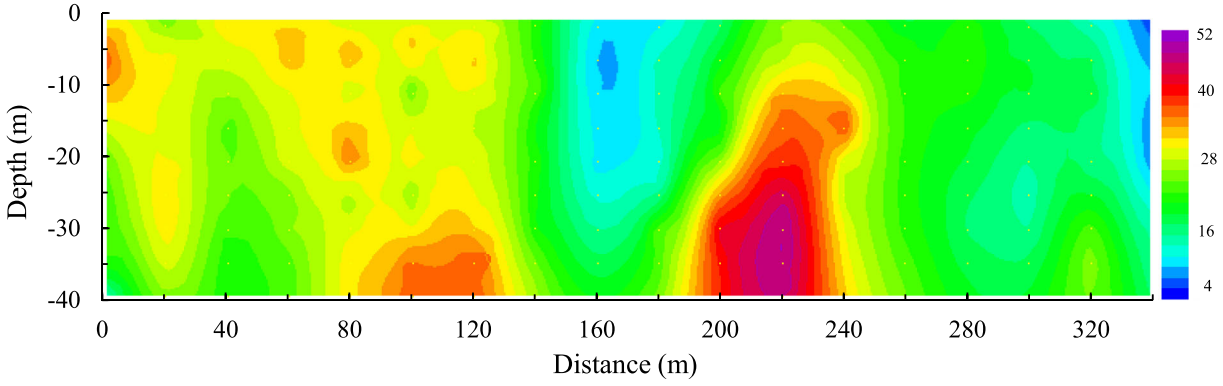

Figure 4. Visualization of fracture frequency (FF) for the profile-section in axis Seyahoo dam.

the core. Encountered FF in these lenses are commonly around 50 f/m, but can locally reach 100 f/m before the rocks disintegrate to breccias. In the surrounding damage zones, networks of fracture sets can be divided into two parts, one made up of fairly high frequencies (20–30 f/m) and the other made up of lower frequencies (<20 f/m). The part with the higher frequencies is mostly found as a narrow zone marginal to the core (inner damage zone), whereas the lower frequency part covers the stretch outwards to background fracture level (outer damage zone). Outcrop studies by Braathen *et al.* (1998) suggest that the high frequency subzone has longer, fault subparallel structures, whereas the latter subzone is characterized by more diverse fracture orientations and lengths. This difference has significant implications for the permeability field in the damage zone because longer fractures will conduct more water than the short ones, due to higher connectivity (Odling 1997). Hence, due to higher frequencies and longer fractures in the inner damage zone the subzone of faults should show higher JH values compared to the outer damage zone.

4.3 *Fault zone permeability*

Packer permeability tests were also carried out to determine the permeability of the rock masses of the dam's abutments and its foundation. The water pressure tests (WPT) were conducted at 586 intervals (including 148 WPT in 18 Exploration boreholes and 438 WPT in 63 Control boreholes) for the drilled boreholes using five-step water pressure loading and unloading (Ewert 1994, 1997b; Kutzner 1996). This process generated five sets of water pressure (P) and water discharge (Q) values, one for each of the five steps. The borehole diameter is 76–86 mm. The tests were carried out with a simple packer system in descending sequence.

Mostly, the test section length ranges from 3.00 to 5.00 m.

The overall differences in structural characteristics between faults in the Seyahoo dam may affect porosity and permeability properties. If this is the case, the faults with narrow cores and less abundant porous fault rock and lower FF in damage zones should in general see less JH. On the contrary, faults with wide cores have both porous breccia and impermeable gouge, as well as higher FF compared to the damage zones. Despite the above-mentioned opposing examples, the general results from this study conformed to the results presented by, for example, Evans *et al.* (1997), which show that the damage zone has the highest permeability (figure 5). Figure 6 visualizes the analyzed data of JH for the profile section of Seyahoo dam axis. When the results of the two faults in Seyahoo dam, as presented in figure 5, are compared, the datasets from the damage zones verify the assumption presented above. There is a slightly higher JH value for damage zones of the F1, with 7–23 Lu (1.2×10^{-4}–4×10^{-4} m^3/s) per fracture compared to 7–18 Lu (1.2×10^{-4}–3×10^{-4} m^3/s) per fracture for F2. Fault core JH is also fairly similar, in the range of 0.5–9 Lu (1×10^{-5}–1.5×10^{-4} m^3/s) per fracture. In other words, the resolution of the datasets (see next

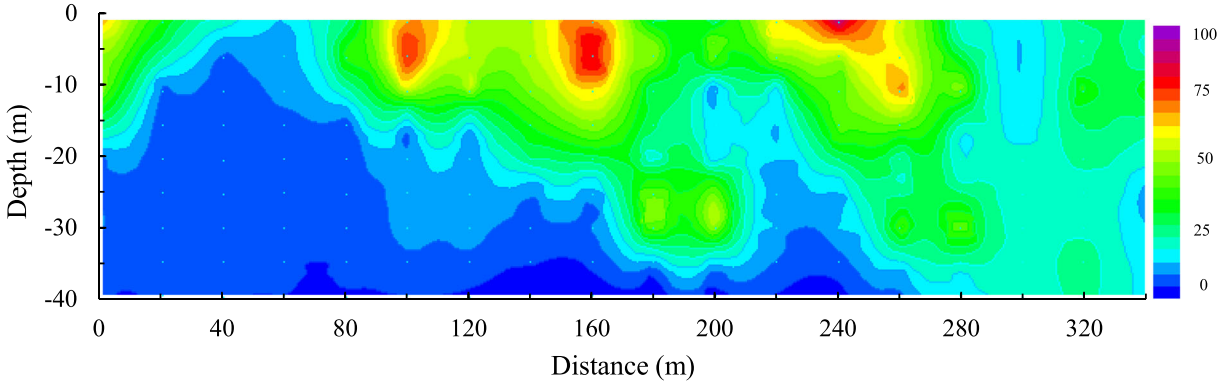

Figure 5. Visualization of Lugeon value (Lu) for the profile-section in axis Seyahoo dam.

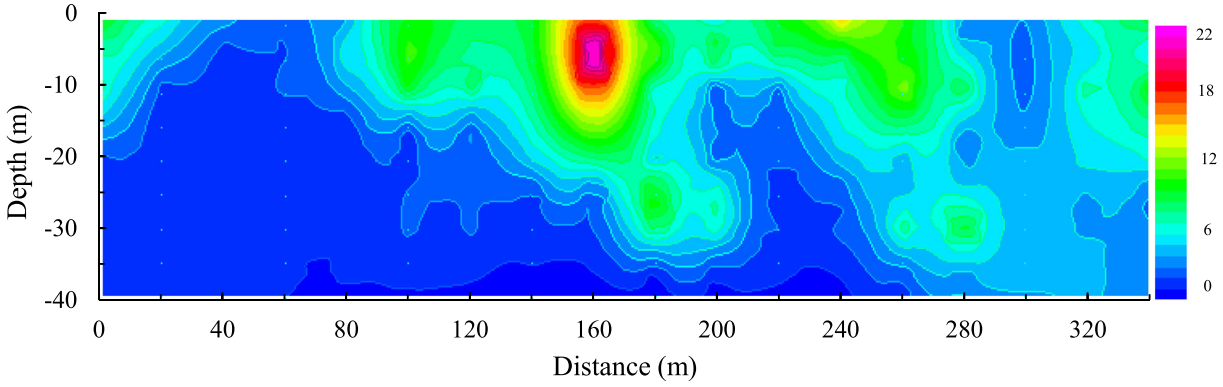

Figure 6. Visualization of joint hydraulic factor (JH) for the profile-section in axis Seyahoo dam.

Table 1. *The amount of JH factor and its characteristics in different subzones: The fault core (C), the inner damage zone (ID) and the outer damage zone (OD) of two faults in the Seyahoo dam.*

	Fault core (C)			Inner damage zone (ID)			Outer damage zone (OD)					
Faults	JH (L/min)	FF (max/m)	Width (m)	JH (L/min)	FF (max/m)	Width (m)	JH (L/min)	FF (max/m)	Width (m)	Ratio (ID/C)	Ratio (OD/C)	Ratio (ID/OD)
F1	0.5–9	60–70	3	14–23	25–45	12–20	7–14	5–15	15	3.9	2.2	1.8
F2	0.5–8	70	2	14–18	30–35	18–25	7–10	10–20	20	4.2	2	1.9
Average	4.5			17			9			4	2	2

paragraph) is not sufficient for the detailed comparison of the permeability characteristics of the individual faults (table 1).

4.4 *Permeability models of faults in crystalline rocks*

Porosity calculations and permeability assessments are generally challenged by the heterogenic nature of fracture aquifers, which will flavor interpretations of injection data in a swarm of drill holes. For example, a single long and highly permeable fracture may conduit cement, and thereby trigger injection in a large volume of porous, fractured rocks. Without this fracture, the volume of available porous rock would be significantly smaller (Danielsen and Dahlin 2006, 2009). Also, the local stress field, which controls fault reactivation and permeability in the fault zone, depends much on the mechanical properties of the rocks that constitute the core and the damage zone. This is analyzed in detail by Gudmundsson *et al.* (2010) who show that the local stresses inside the fault zone can be widely different from those outside the fault zone. However, even with these uncertainties it is likely that large-scale *in situ* JH data better represents rock porosity and permeability fields than the up-scaled result of laboratory measurements of selected structures within major rock zones (Wibberley and Shimamoto 2003), where the flow characteristics of rocks are established through numerical models.

In this dataset (figure 7), the outer damage zone has the average JH of 9.5 Lu (1.6×10^{-4} m^3/s) per fracture, and FF within the range of 5–15 f/m. For the inner damage zone, the JH is in the range of 18 Lu (3×10^{-4} m^3/s) per fracture; with a width of the subzone from 12 to 30 m which has an FF in the range of 25–45 f/m. The average thickness of the fault core is about 2 m, with a peak FF in rock lenses hosted by fault rocks of 60–70 f/m, and an average JH of 3 Lu (5×10^{-5} m^3/s) per fracture. This gives a JH average ratio of inner damage zone and fault core of approximately 4:1, core and outer damage zone ratio of 1:2, and inner and outer damage zone ratio of 2:1.

As outlined, most detailed outcrop studies of fault zones show an increase in FF towards the fault core (figure 8), in some cases even supporting a difference in the fracture distribution between a wider hanging-wall and a narrower footwall (e.g., Caine *et al.* 1996; Braathen *et al.* 1998; Gudmundsson *et al.* 2001; Micarelli *et al.* 2003; Berg and Skar 2005).

4.5 *Resolution in permeability model of faults by JH*

A major challenge in *in-situ* analysis of faults are the different resolutions of available datasets. That is, drill cores (fracture frequency) reveal results on mm to meter scale, whereas permeability data commonly cover intervals on meter-scale. Hydraulic conductivity is significantly affected by fracture

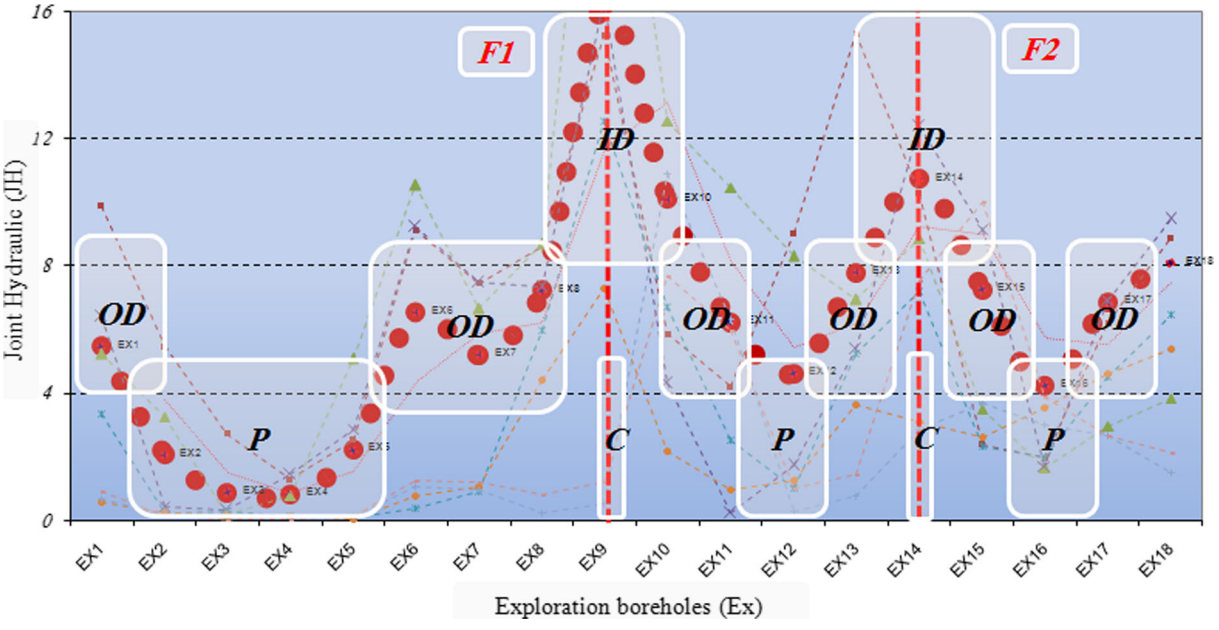

Figure 7. JH distribution correlated with the position of fault rock in Seyahoo dam. The fault zone is divided into subzones (the fault core (C), the inner damage zone (ID), the outer damage zone (OD) and the protolith (P)).

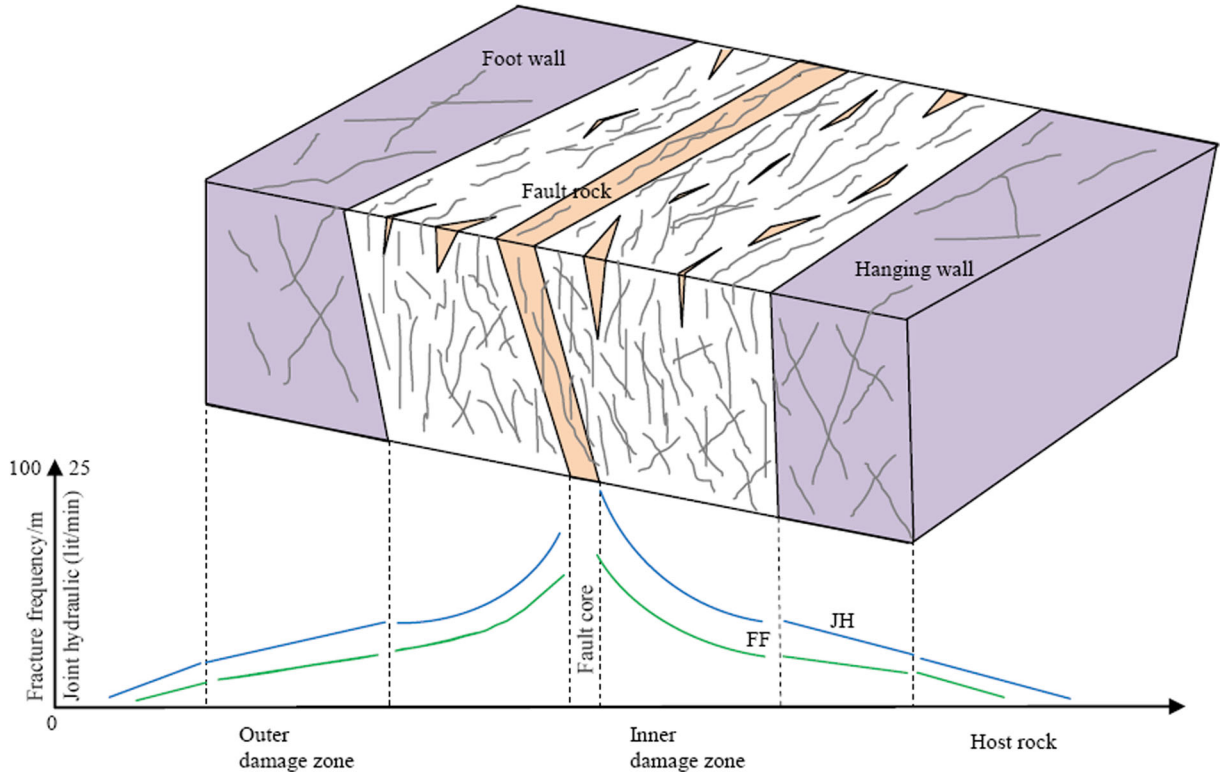

Figure 8. Conceptual model of faults in crystalline rocks, divided into subzones. The curves describe anticipated fracture frequency (FF) of the damage zone and JH factor into the fault zone (the fault core (C), the inner damage zone (ID), the outer damage zone (OD) and the protolith (P)).

networks in crystalline rocks which are characterized by fracture properties. The fracture properties depend on the tectonic history of rocks. It is important to understand the relationship between hydraulic conductivity and the fracture properties to quantify flow in fractured rocks. In this sense, the permeability quality per fracture is defined by the JH.

JH is related to such fracture characteristics as fracture aperture and fracture length, fracture orientation and angle, fracture interconnectivity, filling materials, and fracture plane features. In this model, permeability is related to joint hydraulic factor and the number of conductivity water paths (N_h). Obviously, JH is closely related to the quality of hydraulic per fracture than to the permeability model.

Permeability is expressed in units of length. But in terms of geology, the number of open joints per unit length is different. The present study defines permeability per fracture by JH factor. The JH factor shows the quality of hydraulic and permeability per crack. Understanding JH factor for determining fault zones and treatment by grout is widely used for optimization but the permeability per unit length does not reflect the fracture characteristics.

The core of the fault zone does not cause large inflow, since it usually contains impermeable fault rocks such as gouge (clay rich). Large inflow is commonly found in the damage zone of the fault, where open fractures conduct water. However, the pattern of the significantly increased permeability in the inner damage zone is well documented above, and can be explained by such an empiric model through fracture characteristics as fracture frequency (related by the number of conductive joints (N_h)) and hydromechanical properties of the joint plane (related by JH). In the bounding damage zones, networks of fracture sets make up an inner zone of fairly high JH factor (14–23 Lu) (1.2×10^{-4} – 4×10^{-4} m^3/s) per fracture of fault-parallel, long fractures connected by shorter fractures. An outer zone has lower JH factor (<9 Lu) (1.6×10^{-4} m^3/s) per fracture and more diverse fracture orientations and lengths. This difference has significant implications for the permeability field in the damage zone, since longer fractures will conduct more water than that of short fractures, due to higher connectivity. This sub-zone of faults, therefore, should show higher JH factor values compared to the outer damage zone as a result of higher aperture and longer fractures in the inner damage zone.

Our combined study of quantitative fault zone descriptions, qualitative fracture and fault rock property assessments, as well as JH data sustains the conclusion that there is much more treatment

(cement injected) into the inner damage zone than in the fault core and the outer damage zone.

5. Conclusions

This study of extensional fault zones in Andesite combines datasets from Seyahoo dam, including scan-lines, drill cores, and water pressure test values (WPT). Fault zones show an increase in fracture frequency (FF) from the background fracture level in protolith towards the fault core. Fault zones can be divided into a core, inner damage zone, and outer damage zone based on structural characteristics. There is a substantial increase in JH values in fault zones compared to areas with background fracturing. Fault cores show clear reduction in JH compared to the inner damage zone, possibly caused by abundant impermeable fault rocks in the core. High JH values in the inner damage zone likely relate to a high frequency of long, fault-parallel fractures with good connectivity, whereas lower JH values in the outer damage zone are controlled by lower fracture frequencies (FF) and more variable fracture orientations and lengths. Average JH values of dam for the fault core, the inner damage zone and the outer damage zone are 4, 17, and 9. JH value has a proportionate relationship of 1:4:2 between fault core, inner damage zone, and outer damage zone.

Acknowledgements

The authors would like to express their sincere thanks and profound gratitude to Prof. Nibir Mandal (Associate Editor) and Prof. Agust Gudmundsson for their suggestions and comments for improving this paper. The authors also wish to thank the many engineers, geologists and technical staff of T-Mahar Ab Engineering Company (T-MAECO) and Tamavan Engineering Company (TEC), for providing the field data.

References

Axelsson M and Turesson S 1996 *Injektering med mikrocement, laboratorieförsök och projektutvärdering, Glödbergstunneln, Examensarbete 96/12, Avd för Jord och Bergmekanik*, KTH, Stockholm, Sweden.

Babiker M and Gudmundsson A 2004 The effects of dykes and faults on groundwater flow in an arid land: the Red Sea Hills, Sudan; *J. Hydrol.* **297** 256–273.

Baruah A, Gupta A K, Mandal N and Singh R N 2013 Rapid ascent conditions of diamond-bearing kimberlitic magmas: Findings from high pressure–temperature experiments and finite element modelling; *Tectonophys.* **594** 13–26.

Berg S S and Skar T 2005 Controls on damage zone asymmetry of a normal fault zone: Outcrop analyses of a segment of the Moab fault, SE Utah; *J. Struct. Geol.* **27** 1803–1822.

Blindheim O T and Ovstedal E 2001 Design principles and construction methods for water control in subsea road tunnels in rock; *Norwegian Tunneling Soc.* **12** 43–49.

Braathen A, Gabrielsen R H, Henriksen H, Lothe A, Midtbo E, Midtgård A K, Berg S, Lyslo K and Skurtveit E 1998 *Lineament architecture and fracture distribution in metamorphic and sedimentary rocks with application to Norway;* NGU Report 98.043, Geological Survey of Norway, 78p.

Braathen A, Osmundsen P T and Gabrielsen R H 2004 Dynamic development of fault rocks in a crustal-scale detachment: An example from western Norway; *Tectonophys.* **23** 1–21.

Caine J S, Evans J P and Forster C B 1996 Fault zone architecture and permeability structure; *Geol.* **24** 1025–1028.

Dalmalm T 2004 *Choice of grouting method for jointed hard rock based on sealing time predictions*; Ph.D. thesis, Royal Institute of Technology, Stockholm.

Danielsen B E and Dahlin T 2006 Geophysical and hydraulic properties in rock; Conference processing, 12th European Meeting of Environmental and Engineering Geophysics, 4–6 September 2004, Helsinki, Finland, 4p.

Danielsen B E and Dahlin T 2009 Comparison of geoelectrical imaging and tunnel documentation at the Hallandsas Tunnel, Sweden; *Eng. Geol.* **107** 118–129.

Davoodi M, Jafari M K and Hadiani N 2013 Seismic response of embankment dams under near-fault and far-field ground motion excitation; *Eng. Geol.* **158** 66–76.

Evans J P, Forster C B and Goddard J V 1997 Permeability of fault-related rocks, and implications for hydraulic structure of fault zones; *J. Struct. Geol.* **19** 1393–1404.

Ewert F-K 1994 Evaluation and interpretation of water pressure tests; In: *Grouting in the ground* (ed.) Bell A L, Thomas Telford, London, pp. 141–162.

Ewert F-K 1997a Permeability, groutability and grouting of rock related to dam sites. Part 3: Hydrogeological regimes around dams and reservoirs; *Dam. Eng.* **8** 247–286.

Ewert F-K 1997b Permeability, groutability and grouting of rocks related to dam sites. Part 4: Groutability and grouting of rock; *Dam. Eng.* **8** 271–325.

Faulkner D R and Rutter E H 2001 Can the maintenance of overpressured fluids in large strike-slip fault zones explain their apparent weakness?; *Geol.* **29** 503–506.

Foyo A, Sanchez M A and Tomillo C 2005 A proposal for secondary permeability index obtained from water pressure tests in dam foundations; *Eng. Geol.* **77** 69–82.

Gudmundsson A 2011 *Rock Fractures in Geological Processes*; Cambridge University Press, 592p.

Gudmundsson A, Berg S S, Lyslo K B and Skurtveit E 2001 Fracture networks and fluid transport in active fault zones; *J. Struct. Geol.* **23** 343–353.

Gudmundsson A, Simmenes T H, Larsen B and Philipp S L 2010 Effects of internal structure and local stresses on fracture propagation, deflection, and arrest in fault zones; *J. Struct. Geol.* **32** 1643–1655.

Hoek E 2000 *Rock Engineering-Course*; http://www.rocscience.com.

Hoek E and Bray J W 1981 *Rock Slope Engineering*; 3rd edn, Institute of Mining and Metallurgy, London, 358p.

Karaguzel R and Kilic R 2000 The effect of the alteration degree of ophiolitic mélange on permeability and grouting; *Eng. Geol.* **57** 1–12.

Kutzner C 1996 *Grouting of Rock and Soil*; Balkema, Netherlands, 271p.

Lashkaripour G R and Ghafoori M 2002 The engineering geology of the Tabarak Abad Dam; *Eng. Geol.* **66** 233–239.

Mandal N, Chakraborty C and Samanta S K 2000 Boudinage in multilayered rocks under layer-normal compression: A theoretical analysis; *J. Struct. Geol.* **22** 373–382.

Mandal N, Misra S and Samanta S K 2004 Role of weak flaws in nucleation of shear zones: An experimental and theoretical study; *J. Struct. Geol.* **26** 1391–1400.

Masumoto K, Sugita Y, Fujita T, Martino J B, Kozak E T and Dixon D A 2007 A clay grouting technique for granitic rock adjacent to clay bulkhead; *Phys. Chem. Earth* **32** 691–700.

Micarelli L, Moretti I and Daniel J M 2003 Structural properties of rift-related normal faults: The case study of the Gulf of Corinth, Greece; *J. Geodyn.* **36** 275–303.

Mitchell T M and Faulkner D R 2012 Towards quantifying the matrix permeability of fault damage zones in low porosity rocks; *Earth Planet. Sci. Lett.* **339–340** 24–31.

Mollah M A and Sayed S A S 1995 Assessment of *in situ* permeability with emphasis on packer testing in Kuwait; *Eng. Geol.* **39** 217–231.

Morrow C and Byerlee J 1988 Permeability of rock samples from Cajon Pass, California; *Geophys. Res. Lett.* **15** 1033–1036.

Morrow C and Byerlee J 1992 Permeability of core samples from Cajon Pass scientific drill hole: Results from 2100 to 3500 m depth; *J. Geophys. Res.* **97** 5145–5151.

Morrow C A and Lockner D A 1997 Permeability and porosity of the Illinois UPH 3 drillhole granite and a comparison with other deep drillhole rocks; *J. Geophys. Res.* **102** 3067–3075.

Munier R, Stenberg L, Stanfors R, Milnes A G, Hermanson J and Triumf C-A 2003 *Geological Site Descriptive Model*; SKB Report, R-03-07.

Nonveiller E 1989 *Grouting, Theory and Practice*; Elsevier, Amsterdam, 250p.

Nilsen B and Palmstrom A 2000. *Engineering Geology and Rock Engineering,* Handbook No. 2. Norwegian Group for Rock Mechanics (NBG), 249p.

Norton D and Knapp R 1977 Transport phenomena in hydrothermal systems: The nature of porosity; *Am. J. Sci.* **277** 913–936.

Odling N E 1997 Scaling and connectivity of joint systems in sandstone from western Norway; *J. Struct. Geol.* **19** 1257–1271.

Pollard D D and Aydin A 1988 Progress in understanding jointing over the past century; *Geol. Soc. Am. Bull.* **100** 1181–1204.

Rostami Barani H R 2013 *Present Geological Groutability Index for Rock Mass*; Ph.D. thesis, Ferdowsi University of Mashhad, Iran.

Seront B, Wong T F, Caine J S, Forster C B and Bruhn R L 1998 Laboratory characterization of hydromechanical properties of a seismogenic normal fault system; *J. Struct. Geol.* **20** 865–881.

Shibata I 1981 Procedures for the investigation of permeability and seepage control in soft rock foundations form dams; In: International Symposium on Weak Rock, *in situ* Investigation of the Weak Rock, vol. 1, Balkema, Tokyo, pp. 503–508.

T-Mahar Ab Engineering Company (T-MAECO) 2013 *Engineering Geology Report of Seyahoo Dam Site*; Seyahoo Project, vol. 2, Ministry of Energy, Mashhad, Iran (in Persian).

Walker R J, Holdsworth R E, Armitage P J and Faulkner D R 2013 Fault zone permeability structure evolution in basalts; *Geol.* **41** 59–62.

Wibberley C A J and Shimamoto T 2003 Internal structure and permeability of major strike-slip fault zones: the Median Tectonic Line in Mie Prefecture, southwest Japan; *J. Struct. Geol.* **25** 59–79.

USACE (US Army Corps of Engineers) 1993 *Engineering and Design Seepage Analysis and Control for Dams with CH 1. EM 1110-2-1901*; USACE, Washington DC.

MS received 2 September 2013; revised 13 April 2014; accepted 25 April 2014